IMA Journal of Mathematics Applied in Medicine & Biology (1992) **9**, 177–196

Mathematical models of wound healing in embryonic and adult epidermis

JONATHAN A. SHERRATT

Centre for Mathematical Biology, Mathematical Institute, 24–29 St. Giles', Oxford OX1 3LB, UK

PAUL MARTIN

Department of Human Anatomy, University of Oxford, Oxford OX1 3QX, UK

J. D. MURRAY

Department of Applied Mathematics FS-20, University of Washington, Seattle, Washington 98195, USA

JULIAN LEWIS

ICRF Developmental Biology Unit, Department of Zoology, University of Oxford, Oxford OX1 3PS, UK

[Received 6 July 1992 and in revised form 10 September 1992]

Epidermal wound healing occurs by quite different mechanisms in embryos and adults. In the latter case, it has long been known that cells crawl inwards via lamellipodia to close the defect. In the embryonic system, recent evidence suggests that healing may be caused by a quite different mechanism, namely the contraction of a cable of filamentous actin at the wound edge. The authors use mathematical modelling to investigate both systems. A mechanical model for the initial formation of the actin cable in embryonic epidermal wounds is presented, which incorporates the important phenomenon of stress-induced microfilament alignment. Also discussed is a reaction–diffusion model for the healing of adult wounds subject to auto-regulation of cell division. In both cases, the results suggest possible biological mechanisms for key aspects of the healing process.

Keywords: epidermal wound healing; mathematical modelling; microfilament alignment; growth factors.

1. Mechanisms of epidermal repair in embryos and adults

When adult skin is wounded, the epidermal cells surrounding the lesion crawl inwards to close the defect (Buck, 1979), simultaneously with more complex healing processes in the dermis (Clark, 1989). Although it has long been known that lamellipodial crawling provides the motile force in adult re-epithelialization (Winter, 1962), many aspects of the process remain poorly understood. One major controversy concerns the way in which the movement of the epidermal cell sheet is coordinated. In simpler systems such as amphibian epidermal wound healing, cells in the interior of the sheet

are dragged forward by the pull of the marginal cells (Radice, 1980). However, it remains unclear whether it is this mechanism that operates in mammalian epidermis, or the 'rolling mechanism', in which the leading cells are successively implanted as new basal cells, and other cells roll over these (Krawczyk, 1971; Winstanley, 1975; Stenn & DePalma, 1988). Almost all aspects of adult wound healing are regulated by biochemical growth factors (Martin *et al.*, 1992), and the precise roles of various regulators in epidermal movement is another subject of controversy, which we will discuss in detail below.

Epidermal wound healing in embryos is much less well documented than in adults, but a recent study by Martin & Lewis (1991, 1992) suggests that the processes are quite different in the two systems. Using a tungsten needle, Martin & Lewis made lesions on the dorsal surface of four-day embryonic chick wing buds, by dissecting away a patch of skin approximately 0.5 mm square and 0.1 mm thick. The epidermis, its basal lamina, and a thin layer of underlying mesenchyme were removed. The wounds healed perfectly and rapidly, typically in about 20 hours. Although mesenchymal contraction played some role in healing, the epidermis also moved actively across the mesenchyme; however, there was no evidence of lamellipodia at the wound front in either the basal or superficial (peridermal) layer of the epidermis (Fig. 1). This absence of lamellipodia was consistent with a second observation: when a small island of embryonic skin was grafted onto a denuded region of the limb bud surface, the grafted epidermis, far from expanding over the adjacent exposed mesenchyme, actually contracted, leaving its own mesenchyme exposed. This phenomenon suggested that the mechanism underlying epidermal movement might be a circumferential tension at the free edge, acting like a purse string. Such a

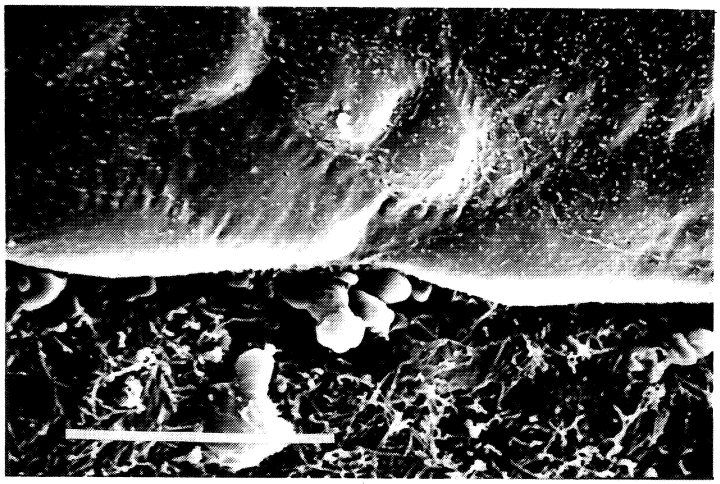

FIG. 1. Scanning electron micrograph of a wound edge in chick embryonic epidermis, 12 hours after the operation. The wound was made by removing a square patch of embryonic skin from the dorsal surface of the wing bud at 4 days of incubation (stage 22/23). The epidermis is above, with the flattened surface of the exposed mesenchyme below. Note the smooth edge of the epidermis and the absence of lamellipodia. A similar absence of lamellipodia is revealed by light microscopy and transmission electron microscopy (Martin & Lewis, 1991). (Scale bar = 10 μm.)

mechanism would cause shrinkage of both an epidermal island and a hole in the epidermis.

Searching for the cause of such a purse string effect, Martin & Lewis (1991, 1992) examined the distribution of filamentous actin in the healing wounds, by staining specimens with fluorescently tagged phalloidin, which binds selectively to filamentous actin (Faulstich *et al.*, 1983; Wulf *et al.*, 1979). This revealed a thick cable of actin around almost all of the epidermal wound margin (Fig. 2), localized within the leading

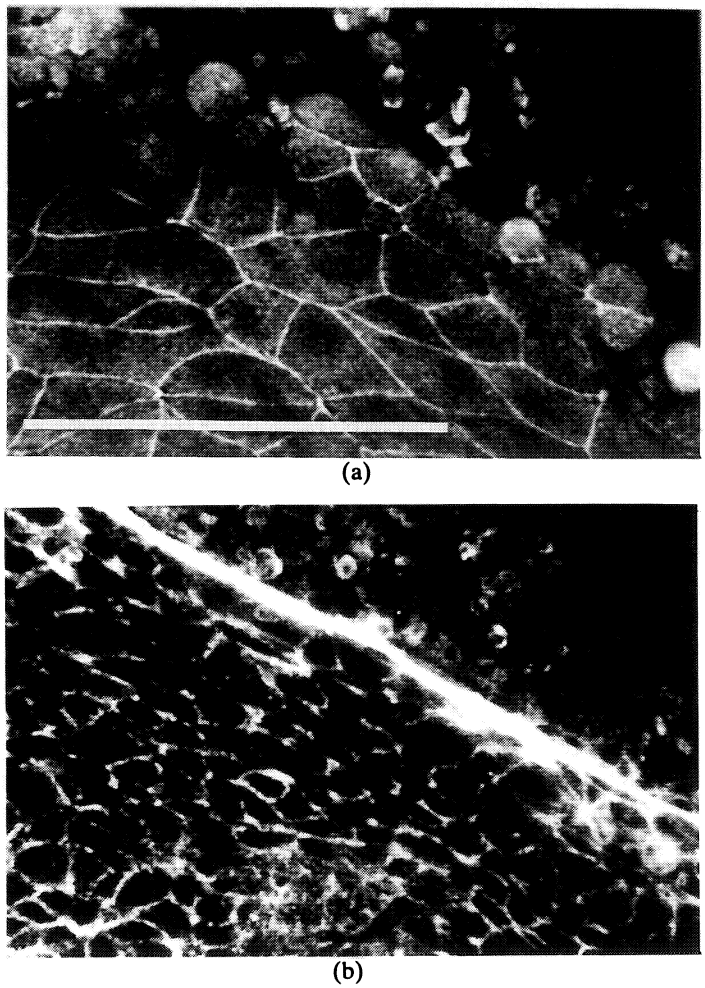

FIG. 2. The epidermal wound front on the dorsum of a chick wing bud after 12 hours of healing, as seen in optical section by confocal scanning laser microscopy. The tissue has been stained with rhodamine-labelled phalloidin, which binds to filamentous actin, and the sections are parallel to the plane of the epidermis. The epidermis is at the lower left, with the exposed mesenchyme (largely below the plane of section) at the upper right. (a) Superficial section, in the plane of the periderm, whose broad flat cells are outlined by their cortical actin. (b) Section about 4 μm deeper, in the plane of the basal epidermal cells, showing the actin cable at the wound front. (Scale bar = 50 μm.)

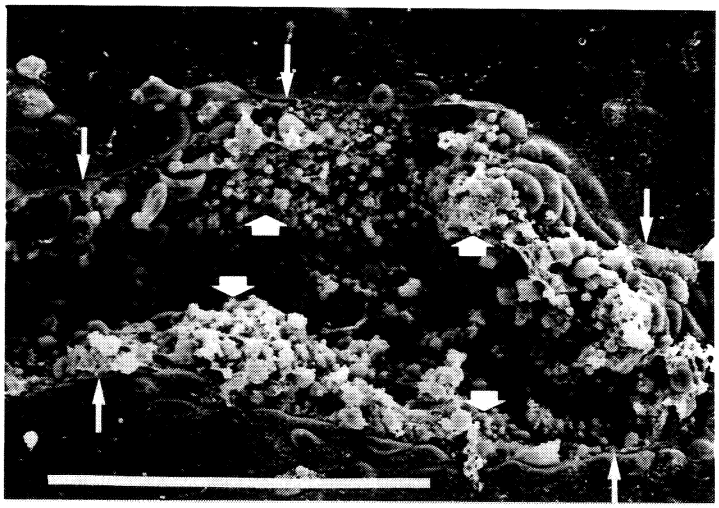

FIG. 3. Scanning electron micrograph of a linear slash wound in chick embryonic epidermis, immediately after the operation. The wound was made on the dorsal surface of the wing bud at 4 days of incubation (stage 22/23). The thin arrows indicate the epidermal wound edge, while the thicker arrows denote the edge of the underlying mesenchyme. The epidermis has retracted over the underlying mesenchyme by about 30–40 μm. (Scale bar = 100 μm.)

row of basal cells. The cable appeared to be continuous from cell to cell, presumably via adherens junctions, except at a very few points; it was present certainly within an hour of wounding, and persisted until the wound was closed. Preliminary evidence suggests that an actin cable may also form at the periphery of the contracting epidermis in the skin grafts discussed above.

To gauge more accurately the time course of the establishment of the actin cable, Midwinter, McCluskey, Martin, & Lewis (in preparation) have investigated simple incisional wounds made by a slash along the proximodistal axis of the limb (Fig. 3). Such a lesion takes only seconds to make, as opposed to the 5–10 minutes required to dissect a square of skin from the limb bud. The slash lesion data indicate that the cells at the wound edge begin to organize their actin into a cable within minutes of wounding, although the cable takes an hour or more to attain its full thickness.

The different mechanisms of healing in adult and embryonic epidermis raise many problems that call for mathematical modelling. Here we discuss models that address two key issues: the formation of the actin cable in embryonic wounds and the role of mitotic upregulation in adult wounds.

2. Actin alignment in embryonic wounds: a mechanical model

The experimental results of Martin & Lewis (1991, 1992) raise two major questions: first, how does the actin cable form, and, second, precisely how does it cause the wound to close, if indeed it has this function? Here we consider the first of these questions. The actin cable forms in response to the creation of a free boundary at the wound edge. We will discuss possible explanations for the aggregation and

pronounced alignment of filamentous actin at the wound edge, which give rise to the actin cable, in terms of a mechanical response to this free boundary.

At the developmental stages we are considering, the embryonic epidermis is two cell layers thick, consisting of a superficial, pavement-like peridermal layer and a cuboidal basal layer. The actin cable develops in the basal layer, and it is to this layer that our modelling considerations apply. The basal cells form a confluent sheet, attached to the underlying basal lamina. Following wounding, the cytoskeleton of these cells undergoes rapid changes, on the time scale of a few minutes (Midwinter *et al.*, in preparation), reaching a new quasi-equilibrium state with a cable of actin at the wound margin. It is this state that we seek to analyse. Of course, this new 'equilibrium' state will change over a time scale of hours, as healing proceeds, but we do not consider here the processes occurring on this longer time scale.

We model the initial response to wounding by amending the mechanochemical model for the deformation of epithelial sheets proposed by Murray & Oster (1984). They treat the epithelium as a linear, isotropic, viscoelastic continuum, an approach which is discussed from a rheological viewpoint by Elson (1988). We amend this model to investigate the new equilibrium reached by the basal cell sheet after wounding. Viscous effects can be neglected since we are only interested here in the short term 'equilibrium' state, and this simplifies the model. However, an important addition to the Murray–Oster model will be the effects of a microfilament anisotropy, which plays a crucial role in our system.

The mechanical properties of a confluent cell sheet are determined largely by the intracellular actin filaments (Pollard, 1990). In epithelial sheets, cell–cell adherens junctions serve as connection sites for actin filaments, and thus the intracellular actin filaments are linked, via transmembrane proteins at these junctions, in an effectively two-dimensional transcellular network. Our model addresses the equilibrium state of this network. The forces exerted on an epidermal cell by the epidermal cells around it, via this actin filament network, can be divided into two types: elastic forces and active contraction forces; we include the effects of osmotic pressure within 'contraction forces' (Oster, 1984). The elasticity of the actin filament network arises from the extensive interpenetration of the long actin filaments, which tends to immobilize them (Janmey *et al.*, 1988). The exertion of cellular traction forces has been extensively studied for fibroblasts (see e.g. Harris, 1982; Stopak & Harris, 1982), and traction forces have been observed in a range of other cell types, including chick embryonic corneal epithelial cells (Mattey & Garrod, 1984).

At equilibrium, these elastic and traction forces balance the elastic restoring forces that arise from attachment to the mesenchyme. Thus, the model equation, which predicts the new equilibrium configuration attained by the actin filament network of the epidermis after wounding, has the following form:

Elastic forces within the actin filament network	+	Traction forces exerted by actin filaments	=	Elastic restoring forces due to substratum attachments

This force balance is illustrated in Fig. 4. The mathematical formulation of the equation is discussed briefly in Appendix A, and will be published in more detail elsewhere. A crucial feature of this formulation is the relationship between the density

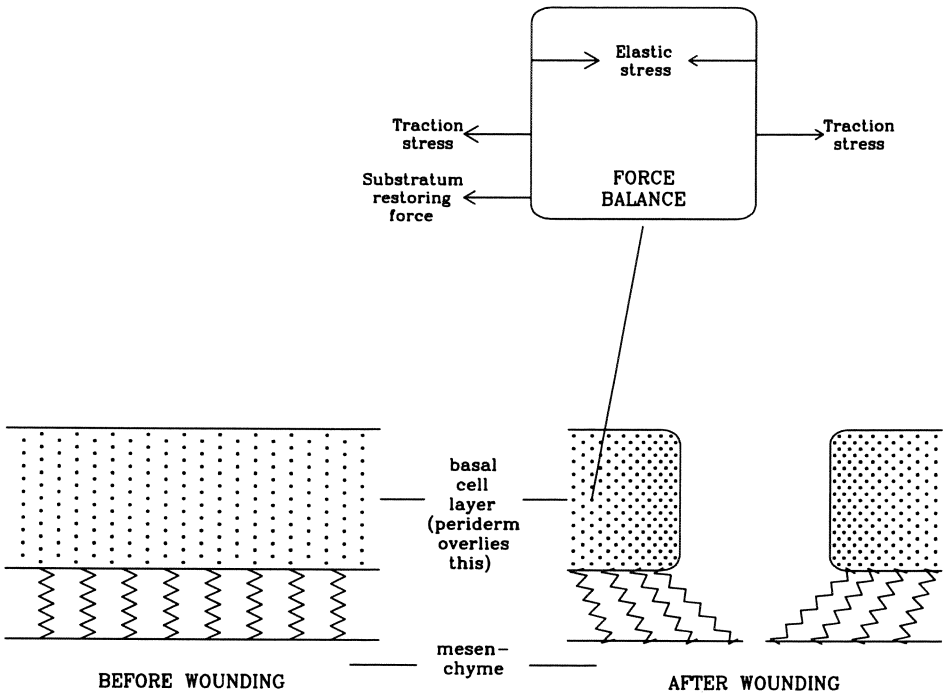

FIG. 4. A schematic representation of the force balance in the basal cell sheet. Following wounding, the epidermis retracts relative to the underlying mesenchyme, until a mechanical equilibrium is reached. Elastic and traction stresses are exerted by the surrounding cells at each point in the sheet, and in the post-wounding equilibrium, these elastic and traction forces balance the restoring forces due to substratum attachments. The movement of the 'springs' represents local deformation of the superficial mesenchyme due to tension in the epidermis. In reality, the mesenchyme and epidermis are separated by a basal lamina, and our modelling assumes that the attachments are fixed in the basal lamina, and that this becomes wrinkled (so that the attachments are compressed) in response to wounding, to an extent reflecting the compaction of the cell sheet.

of microfilaments at a point, and the amount of expansion or compression of the tissue resulting from the displacements of that and neighbouring points from their initial positions. This relationship is implied by our assumption that, in the response to wounding, the amount of filamentous actin in each basal cell remains constant.

When appropriately nondimensionalized, the mathematical formulation of the model involves four parameters. Two of these reflect the mechanical properties of the microfilament network in the epithelium, and another represents the extent to which displacements of the epithelium are resisted by its tethering to the underlying mesenchyme. The fourth parameter β reflects the extent to which compaction of the actin filament network increases the traction stress exerted per filament. Such a synergy phenomenon is intuitively expected to some extent: actin filaments together exert a greater traction force than the sum of the traction forces they exert separately, since as the degree of filament overlap increases, additional myosin cross-bridges form (Oster & Odell, 1984). As in other applications of mechanochemical models, the

experimental data available to give estimates for parameter values is still limited, and is in this case insufficient to determine any of these quantities.

2.1 *Stress-induced alignment of actin filaments*

A further important feature of our mathematical model is that it incorporates the phenomenon of stress alignment of actin filaments. That is, when a mesh of actin filaments is subjected to a stress field, the filaments tend to align the directions of maximum stress. We now briefly review the experimental evidence for this phenomenon. The seminal paper is a study involving micromanipulation of fish epidermal cells by Kolega (1986). He found that in a cell held under tension either by micromanipulation or by cellular locomotive activity, actin filaments were aligned parallel to the tension. Moreover, when the tension was due to micromanipulation, filament alignment occurred as a direct response to the applied tension, within a few seconds.

In a previous but quite similar study, Chen (1981) applied micromanipulation to chick heart fibroblasts. His observations of the cytoskeleton suggest that the actin filament network is rather like a three-dimensional fish net under tension, with its fibres oriented along directions of stress. A similar analogy is used by Kolega (1986). However, it is important to emphasize that stress alignment of actin is not simply like the passive stress alignment of a fish net, but almost certainly involves the breaking and making of actin filament attachments. Chen (1981) found that upon detachment of a fibroblast tail from the substratum, with consequent reduction of the stress in the cytoskeleton, the microfilament bundles lost their orientation and reassumed a random meshwork arrangement, over a time scale of about 15 seconds; thus the observed filament alignment is dependent on stress in the elongated tails.

Valberg & Albertini (1985) exerted forces on pulmonary macrophages from the lungs of hamsters by causing the macrophages to ingest magnetic particles, and applying external magnetic fields. They found prominent patches of positive staining for actin coinciding with the location of the particles, aligned with the magnetic force field. These observations again suggest alignment of actin filaments along directions of stress. Finally, there is a considerable body of literature on stress-induced alignment of 'stress fibres', that is actin filament bundles, both in fibroblasts attached to substratum (Trinkaus, 1984; Bershadsky & Vasiliev, 1988) and in endothelial cells under shear stress, which is an important feature of blood flow (see e.g. Wechezak *et al.*, 1985, 1989).

The actin cable consists of an aggregation of microfilaments at the wound edge, all aligned parallel to this edge. The above experimental evidence suggests that this alignment could be a direct result of the anisotropic stress field near the wound edge, which results from this edge being a free boundary. To incorporate this phenomenon of stress-induced alignment in our model, we take the proportion of actin filaments aligned parallel to the wound edge to be an increasing function of the ratio of the components of the stress field parallel and perpendicular to the wound edge. The mathematical details of this approach are discussed in Appendix A, and in more detail by Sherratt & Lewis (1992).

2.2 *Solutions of the model*

As discussed above, the most detailed quantitative data on the initial response of embryonic epidermis to wounding is from slash wound experiments. To simulate these wounds, we solved the model equilibrium equation in a one-dimensional geometry. As discussed in Appendix A, the equation then has a solution provided the parameter values are restricted to a well-defined parameter domain. For parameter values near one edge of this domain, the model solutions exhibit both an intense aggregation of filamentous actin at the wound edge, and pronounced alignment of these aggregated filaments with the wound edge, as illustrated in Fig. 5. Moreover, for appropriate parameter values, the model solutions also predict a similar degree of retraction of the epidermis over the underlying mesenchyme to that found experimentally, namely about 30–40 μm (Figs. 3 and 6). To better illustrate the correspondence between the predicted actin filament density and the experimental results of Martin & Lewis (1991, 1992), we used the model solutions to simulate an optical section through the basal layer of the epidermis of a specimen stained with fluorescently labelled phalloidin. To do this, we treated the filamentous actin distribution predicted by the model, appropriately normalized, as an intensity distribution for phalloidin staining. Our simulation is shown in Fig. 7; it compares well with the corresponding experimental result (Fig. 2B).

Our modelling suggests that the initial formation of the actin cable in embryonic epidermal wounds may occur simply as a by-product of the post-wounding mechanical

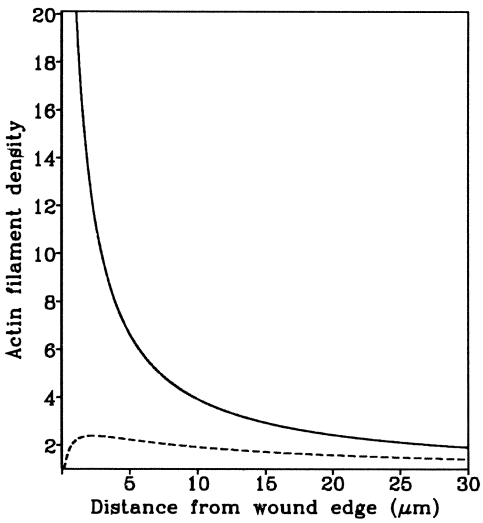

FIG. 5. The density of actin filaments aligned parallel (——) and perpendicular (– – – – –) to the wound edge, per unit area of the microfilament network, in response to a linear slash wound, as predicted by the model, for parameter values close to the edge of the parameter domain in which a solution exists. Distance orthogonal to the wound edge is plotted horizontally, and actin filament density is expressed relative to the (uniform) pre-wounding density. The dimensionless elasticity and adhesion parameter ratios are, in terms of the dimensional parameters described in Appendix A, $\lambda L^2/\tau_0 = 3.0$, $E/\tau_0 = 0.2$, $\Gamma/\tau_0 = 0.75$, $\beta = 0.16$, where the length scale $L = 500$ μm.

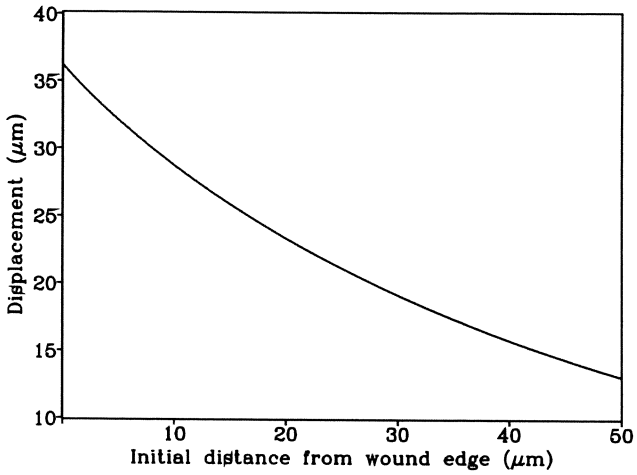

FIG. 6. The displacement of the epidermal cell sheet from its pre-wounding position in response to a linear slash wound, as predicted by the model. The predicted displacement of the wound edge (36 μm) is roughly the same as that observed experimentally (see Fig. 3). Analytical investigation of the model equations, which is discussed in detail by Sherratt (1992a), shows that, as expected intuitively, the displacement of the wound edge increases as the elasticity parameters E and Γ increase, and decreases as the adhesion and traction parameters λ and τ_0 are increased. The dimensionless elasticity and adhesion parameter ratios are, in terms of the dimensional parameters described in Appendix A, $\lambda L^2/\tau_0 = 3.0$, $E/\tau_0 = 0.2$, $\Gamma/\tau_0 = 0.75$, $\beta = 0.177$, where the length scale $L = 500$ μm. These parameter values are close to the edge of the parameter domain in which a solution exists.

equilibrium in the epidermal cell sheet. Central to the formation of the cable is the phenomenon of stress-induced actin filament alignment, as illustrated in Fig. 8. This alignment phenomenon may play an important part in a number of processes in normal morphogenesis, such as convergent extension (Gerhart & Keller, 1986; Lewis, Jesuthasan, & Sherratt, in preparation). Because oriented actin filaments themselves actually generate stress, alignment can arise spontaneously in these cases through positive feedback (Sherratt & Lewis, 1992); the response to wounding represents a rather different case, in which alignment is caused by a change in external conditions, namely the generation of a free edge by wounding.

3. Growth factors in adult wounds: a reaction–diffusion model

The complex healing processes in both the dermis and epidermis of adult mammalian skin are closely regulated by biochemical growth factors (see Martin *et al.*, 1992, for a review). Many of these growth factors are released during the initial inflammatory response to injury, while others are released gradually throughout healing. In epidermal repair, the growth factor profile regulates two processes in particular: cell motility and cell proliferation. This biochemical regulation is amenable to theoretical investigation via reaction–diffusion models. Here we focus on mitotic control, and briefly review the work of Sherratt & Murray (1990, 1991, 1992a,b).

Cells in unwounded epidermis are nonmotile, but in the neighbourhood of a wound

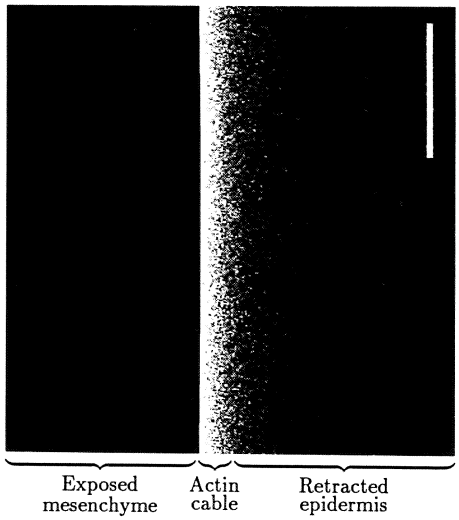

FIG. 7. A simulation of an optical section through the basal layer of the epidermis in response to a circular wound of radius 500 μm, after staining with fluorescently labelled phalloidin, as predicted by the model solutions. We treat the filamentous actin distribution predicted by the model, appropriately normalized, as a probability distribution for phalloidin staining. The figure shows nine million points, with radial coordinate chosen at random from this distribution, and angular coordinate chosen at random from a uniform distribution. The dimensionless parameter ratios are, in terms of the dimensional parameters described in Appendix A, $\lambda R^2/\tau_0 = 1.5$, $E/\tau_0 = 0.29$, $\Gamma/\tau_0 = 0.77$, $\beta = 0.2876$, where R is the initial wound radius. (Scale bar = 10 μm.)

they undergo a marked phenotype change, permitting lamellipodial crawling (Gabbiani *et al.*, 1978). *In vitro* studies suggest that this lamellipodial activity is regulated by biochemicals such as epidermal growth factor (Barrandon & Green, 1987). However, the model we will discuss glosses over the subtleties of such regulation in order to focus instead on mitotic control; for in adult wounds, which are generally much larger than the embryonic wounds discussed above, large numbers of new cells have to be generated if the lesion is to heal. This is not to say that regulated motility is not an important feature of epithelial healing—indeed, it is essential. But we represent the effects of motility here in the simplest possible way, as a diffusional migration of cells down the gradient of cell population density. By adopting this (perhaps oversimplified) background assumption, we are able to compute the proliferative behaviour of the cells, which we take to be regulated by cell population density and by a diffusible factor that the cells secrete. We use our model to investigate how the parameters of mitotic control might affect the rate of wound closure, and to examine whether they can account for some striking features of the observed time course of healing.

Homeostasis in normal epidermis is achieved by a combination of biochemical activators and inhibitors of cell division (Watt, 1988a,b). This control mechanism ensures a rapid increase in mitosis following injury, by as much as fifteen times (Winter, 1972; Danjo *et al.*, 1987); its breakdown can lead to malignancies (Weinberg, 1989; Sherratt, 1992b; Sherratt & Nowak, 1992). Many regulators of epidermal mitosis are produced in the underlying connective tissue. However, some growth

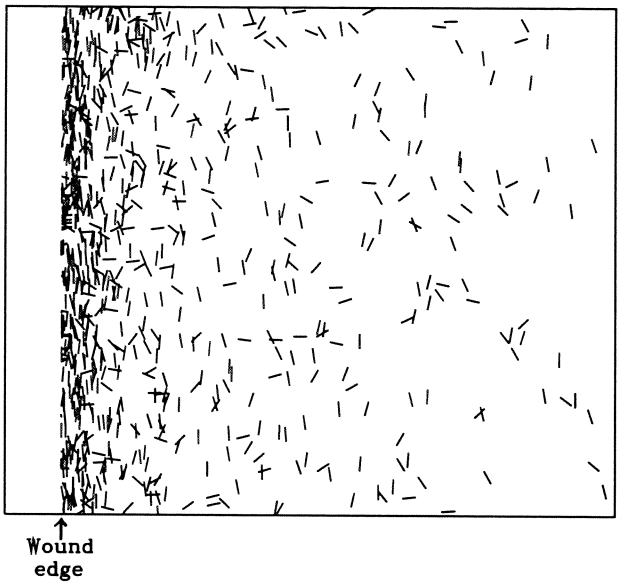

FIG. 8. An illustration of the stress-induced preferential alignment of the microfilament network in response to a linear slash wound, as predicted by the model solutions. We treat the filamentous actin distribution predicted by the model, appropriately normalized, as an intensity distribution for the location of small line segments. The figure shows 800 such line segments, centred at a point whose orthogonal distance from the wound edge is chosen at random from this distribution, with position parallel to the wound edge chosen at random from a uniform distribution. The orientation of the line segments is chosen at random from the distribution F of actin filament orientations, which is discussed in Appendix A. The dimensionless parameter ratios are, in terms of the dimensional parameters described in Appendix A, $\lambda L^2/\tau_0 = 3.0$, $E/\tau_0 = 0.26$, $\Gamma/\tau_0 = 0.7$, $\beta = 0.22$, where the length scale $L = 500\ \mu m$.

regulators may be produced in an autocrine fashion by the epidermal cells themselves, and a number of auto-activators and auto-inhibitors of epidermal mitosis have recently been characterized (Elgjo *et al.*, 1986a,b; Coffey *et al.*, 1987; Halaban *et al.*, 1988). For simplicity, we consider the case of a single mitotic regulator, which can be either an activator or an inhibitor of cell division, and which is produced by the keratinocytes. Conservation equations for this system have the following form:

Rate of increase of cell density	=	Cell migration	+	Chemically controlled mitotic generation	−	Natural loss (sloughing)
Rate of increase of chemical concentration	=	Diffusion	+	Production by cells	−	Decay of active chemical

We take the mitotic rate to be an increasing function of chemical concentration in the activator case, and a decreasing function in the inhibitor case. Similarly, the rate of chemical production by cells increases for a mitotic inhibitor, and decreases for an activator. In Appendix B we discuss the mathematical formulation of these equations as a reaction–diffusion system.

A feature common to almost all experimental studies of epidermal wound healing is the biphasic nature of the healing process: a lag phase, comprising about 10%

of the healing time for typical wound dimensions, followed by a linear phase in which the cell front advances with constant speed (Crosson *et al.*, 1986; Frantz *et al.*, 1989). With parameter values based as far as possible on experimental data (Sherratt & Murray, 1990), our model is able to capture this key aspect of the healing process in both the activator and inhibitor cases (Figs. 9 and 10). Moreover, solutions of the model equations for a variety of different wound shapes suggest a possible mechanism for the control of changes in wound shape during healing, and suggest that it may be possible to distinguish between the activator and inhibitor mechanisms by examining the variations in healing time with wound shape (Sherratt & Murray, 1992b). The model can also be used to make quantitative predictions concerning the

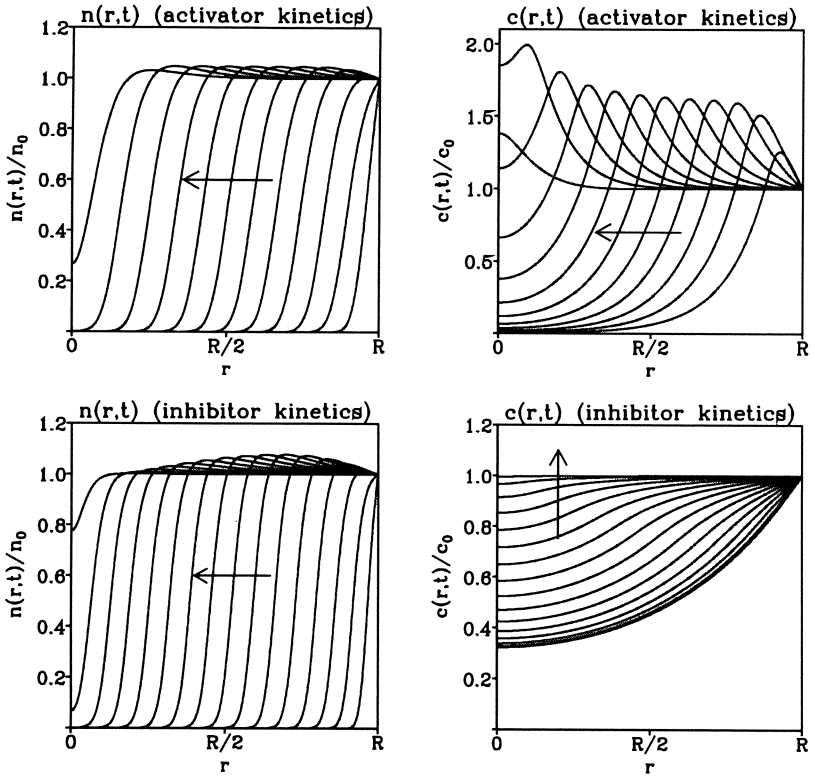

FIG. 9. Typical solutions of the model equations (B.1) for a circular wound in adult epidermis, with both activator and inhibitor kinetics. We plot cell density and chemical concentration as a function of radius r at equally spaced times; the arrows indicate the way in which the solution changes as t increases. As expected intuitively, the solutions consist of a wave of cell density moving inwards to close the wound, with an associated wave of chemical concentration; in one spatial dimension, corresponding to a simple incisional lesion, the solutions are qualitatively very similar, and are amenable to analysis as travelling waves (Sherratt & Murray, 1991). The dimensionless parameter ratios are as follows, in terms of the dimensional parameters described in Appendix B: in the activator case $D/kR^2 = 5 \times 10^{-4}$, $D_c/kR^2 = 0.45$, $\lambda/k = 30$, $h = 10$, $c_m/c_0 = 40$, $\alpha/n_0 = 0.1$, and in the inhibitor case $D/kR^2 = 10^{-4}$, $D_c/kR^2 = 0.85$, $\lambda/k = 5$, $h = 10$; R is the initial wound radius. These parameter values are based on experimental data, as discussed by Sherratt & Murray (1990, 1992a).

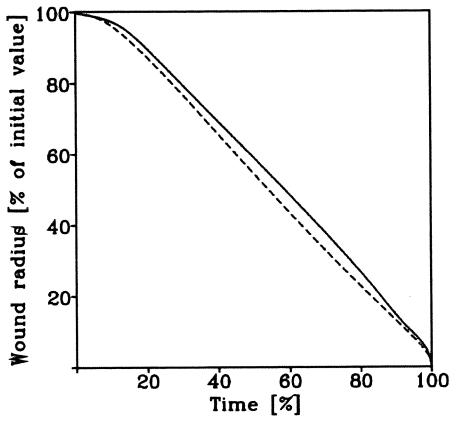

FIG. 10. The decrease in wound radius with time for a circular wound in adult epidermis, as predicted by the model (B.1). These healing profiles are derived from the solutions shown in Fig. 9, by taking the wound edge as the contour $n/n_0 = 0.8$; the curves are not sensitive to the choice of contour level. These curves demonstrate that the model solutions capture the biphasic nature of re-epithelialization: a lag phase followed by a linear phase. The parameter values are as in Fig. 9; —— activator kinetics, – – – – – inhibitor kinetics.

acceleration of healing by the topical application of mitotic activators, which has been observed experimentally (Eisinger *et al.*, 1988; Madden *et al.*, 1989; Sherratt & Murray, 1992b).

Our modelling suggests that biochemical auto-regulation of mitosis can promote epidermal wound healing by providing a new population of cells in the advancing front. Moreover, both activation and inhibition of mitosis can explain the experimentally observed biphasic nature of the healing process; in contrast, a reaction–diffusion model without mitotic auto-regulation fails to capture this central phenomenon (Sherratt & Murray, 1990). These results support the view that biochemical control of mitosis plays a major role in re-epithelialization; however, they do not rule out an important role for activation of cell motility by growth factors, or exclude mechanisms of wound closure such as that described in the first half of this paper.

4. Conclusions

Epidermal wound healing provides a rich source of modelling opportunities. Here we have focused on two key issues: the mechanism of formation of the actin cable in the embryonic system, and the role of biochemical control of mitosis in adult epidermis. These very different problems require different types of model: in the former case, a mechanical model representing the force balance in the cytoskeleton, and in the latter a reaction–diffusion model for the conservation of cells and growth factors as the wound front advances. These two models do not represent mutually exclusive concepts of the way wounds heal; rather, they deal with different aspects of this complex process. Nevertheless, the two models draw attention to some marked

differences between embryonic and adult epidermal healing. Certainly the motile force in adult epidermal wound healing is not provided by an actin cable, and the process of lamellipodial crawling prohibits the existence of a permanent cable around the wound margin. However, there may be relatively short and transient actin cables at parts of the wound edge, as at free edges of epithelia *in vitro* (Vaughan & Trinkaus, 1966; DiPasquale, 1975a, b): to our knowledge, this has not been investigated experimentally. Conversely, embryonic cells are competent to crawl via lamellipodia, since wounds in embryonic sheets *in vitro* heal by crawling rather than by a purse string mechanism (Hergott *et al.*, 1989). As for the role of mitotic control in embryonic versus adult wound healing, important differences may arise from differences in the sizes of the lesions one is dealing with, as discussed earlier. Another significant difference is that growth factor levels appear to be much lower in foetal wounds (Whitby & Ferguson, 1991), and recent experiments suggest that these lower growth factor concentrations may be responsible for at least one major contrast between wound healing in adults and foetuses, namely the scarless healing of foetal wounds (Shah *et al.*, 1992). But that phenomenon, hinging on the behaviour of the connective tissue in the healing wound, would call for yet another sort of mathematical model.

Appendix A

Here we briefly describe the mathematical formulation of the modelling considerations discussed above for the formation of the actin cable in embryonic epidermis. More details of the mathematics appear elsewhere (Sherratt & Lewis, 1992; Sherratt, 1991, 1992a). As described in the main body of the paper, when a microfilament network is subject to a nonisotropic stress field, the filaments tend to align along the directions of maximum stress. In the absence of detailed information on the biological mechanisms responsible for this stress alignment, we develop a model for the phenomenon by making a number of intuitively plausible assumptions. Most importantly, we assume that the alignment occurs as a direct response to the ratio of the principal components of stress, σ_1 and σ_2 say. Then the effective densities of actin filaments aligned along the principal axes of stress are

$$G_1 = G_0 \int_0^{\pi/2} F(\phi; \sigma_1/\sigma_2) \cos\phi \, d\phi, \qquad G_2 = G_0 \int_0^{\pi/2} F(\phi; \sigma_1/\sigma_2) \sin\phi \, d\phi,$$

where $G_0(\boldsymbol{r})$ is the local 'scalar' actin filament density, and $F(\phi; \sigma_1/\sigma_2)\,\delta\phi$ is the fraction of actin filaments at the point concerned that are oriented at an angle between ϕ and $\phi + \delta\phi$ to the 1-axis, for a given ratio of the principal components of stress. We require that the function F satisfies the following conditions:

(i) $F(\phi; 0) = \delta(\phi)$: when the stress is unidirectional, all the actin filaments are oriented in that direction. (Here δ denotes the Dirac delta-function).
(ii) $F(\phi; 1)$ is constant: when the stress is isotropic, the microfilament network is randomly oriented.
(iii) $\int_0^{\pi/2} F(\phi; \sigma_1/\sigma_2)\, d\phi = 1$ for all σ_1 and σ_2: filament alignment does not affect the total amount of filamentous actin.
(iv) $F(\phi; \sigma_1/\sigma_2) = F(\frac{1}{2}\pi - \phi; \sigma_1/\sigma_2)$: a symmetry condition.

These conditions do not determine a specific form for F. However, they are highly restrictive, and Sherratt & Lewis (1992) have developed a form for F which satisfies these conditions, and have shown that this implies that, to a good approximation,

$$\int_0^{\pi/2} F(\phi; \sigma_1/\sigma_2) \cos\phi \, d\phi = \frac{\pi\sigma_1^p}{2\sigma_1^p + (\pi - 2)\sigma_2^p}.$$

The positive parameter p reflects the sensitivity of the microfilament network to changes in the stress field. Here we assume that $p = 1$ for algebraic simplicity. Then, in the post-wounding equilibrium we are considering, the principal components of the stress tensor in the cell sheet are given by

$$\left.\begin{aligned} \sigma_1 &= G_1[E\varepsilon_1 + \Gamma\nabla\cdot\boldsymbol{u}] + G_1\tau, \\ \sigma_2 &= \underbrace{G_2[E\varepsilon_2 + \Gamma\nabla\cdot\boldsymbol{u}]}_{\text{elastic stress}} + \underbrace{G_2\tau}_{\text{active contraction stress}}, \end{aligned}\right\} \tag{A.1}$$

where $G_1 = G_0\pi\sigma_1/[2\sigma_1 + (\pi - 2)\sigma_2]$ and $G_2 = G_0\pi\sigma_2/[2\sigma_2 + (\pi - 2)\sigma_1]$. Here, $\boldsymbol{u}(\boldsymbol{r})$ is the displacement of the material point initially at $\boldsymbol{r}$, ε_1 and ε_2 are the principal components of the strain tensor $\boldsymbol{\varepsilon} = \frac{1}{2}(\nabla\boldsymbol{u} + \nabla\boldsymbol{u}^{\mathrm{T}})$, and E and Γ are positive constants. The stress and strain tensors $\boldsymbol{\sigma}$ and $\boldsymbol{\varepsilon}$ have the same principal axes. As discussed above, the traction stress per filament, τ, is in general a function of the compaction of the actin filament network, and we take $\tau = \tau_0/(1 - \beta\Omega)$, where τ_0 is a positive constant and Ω is the fraction of its pre-wounding area by which a small region of the actin filament network contracts after wounding. The biological interpretation of the parameter β has been discussed in detail in the main body of the paper. Although our modelling of actin filament alignment is novel, the representation of the elastic and traction components of the stress tensor in (A.1) is used extensively in the literature: see, for example, Oster *et al.* (1983), Murray & Oster (1984), Oster (1984), Oster *et al.* (1985), Murray *et al.* (1988), or, for a detailed review, Murray (1989). In contrast to the majority of these models, (A.1) has no viscous contribution because we are considering the equilibrium situation. Also, we do not include an osmotic pressure term since, in the absence of chemical control, such a term would simply have the form of a negative traction (Oster, 1984). Following Murray & Oster (1984) again, we model the restoring forces due to substratum attachment by $\lambda G_0\boldsymbol{u}$, where the positive constant λ reflects the strength of these attachments. The dependence on G_0 arises because we assume that the attachments are fixed in the basal lamina and that this becomes wrinkled (so that the attachments are compressed) in response to wounding, to an extent reflecting the compaction of the cell sheet. Direct experimental evidence for this dependence is given by Hergott *et al.* (1989) and Wechezak *et al.* (1989).

Thus the equation to be solved for the post-wounding equilibrium configuration is

$$\nabla\cdot\boldsymbol{\sigma} - \lambda G_0\boldsymbol{u} = \boldsymbol{0}, \tag{A.2}$$

with $\boldsymbol{\sigma}$ given by (A.1). Our assumption that the amount of filamentous actin in a

given region of the basal cell sheet remains constant as that region is deformed implies that $G_0(1 - \Omega)$ is constant. We treat the cell sheet as infinite, which is valid provided the wound area is small compared to the whole sheet; this certainly holds in the experiments we are modelling. Thus the boundary conditions are $\boldsymbol{u}(\infty) = \mathbf{0}$ and $\boldsymbol{\sigma}\cdot\hat{\boldsymbol{n}} = \mathbf{0}$ at the free edge, where $\hat{\boldsymbol{n}}$ is the unit vector normal to this edge: as discussed above, we treat the actin filament network as two dimensional.

Sherratt (1992a) has shown that, with these boundary conditions, (A.2) has a solution in one spatial dimension, corresponding to a linear slash wound, if and only if the parameter values satisfy either $2E/(4 - \pi) + \Gamma - 1/(1 - \beta) > 0$ with $\beta \leqslant \frac{1}{2}$ or $2E/(4 - \pi) + \Gamma - 4\beta \geqslant 0$ with $\beta > \frac{1}{2}$. Moreover, as $2E/(4 - \pi) + \Gamma - 1/(1 - \beta) \to 0^+$ with $\beta < \frac{1}{2}$, the density at the wound edge of filamentous actin aligned parallel to that edge tends to infinity, so that the model solution reflects the phenomenon of the actin cable for parameter values close to this edge of the parameter domain.

Appendix B

In this appendix we briefly discuss the mathematical formulation of the reaction–diffusion model discussed above for adult epidermal wound healing controlled by a single mitotic regulator. The governing equations represent local conservation of cell density and chemical concentration as the wound front advances. We represent cell migration by simple linear diffusion, and take chemical decay and natural cell loss as first-order processes. The mitotic regulator is produced by the epidermal cells themselves, at a rate that varies with the local cell density. Denoting the cell density by $n(x, t)$, with x the spatial coordinate and t the time variable, we represent the rate of chemical production as $f(n)$. We take the mitotic rate per cell to be given by $s(c)(2 - n/n_0)$, where $c(x, t)$ is the chemical concentration and n_0 is the cell density in unwounded epidermis; this form reflects both chemical control and a decrease in proliferation due to crowding.

The dimensional model equations are thus

$$\left.\begin{aligned} \frac{\partial n}{\partial t} &= D\nabla^2 n + ns(c)(2 - n/n_0) - kn, \\ \frac{\partial c}{\partial t} &= D_c\nabla^2 c + f(n) - \lambda c. \end{aligned}\right\} \tag{B.1}$$

Here D and D_c are the cell and chemical diffusion coefficients, and the positive constants k and λ are the rate constants of cell loss and chemical decay. It remains to discuss the forms of $f(n)$ and $s(c)$. If c_0 is the unwounded chemical concentration, we require $s(c_0) = k$ and $f(n_0) = \lambda c_0$ so that the unwounded state is an equilibrium state of the model. Further, in the inhibitor case, $s(c)$ must be a decreasing function with $f(n)$ increasing. For a mitotic activator, $s(c)$ is increasing, and we take $f(n)$ to increase rapidly from zero before decreasing gradually—we require $f(0) = 0$ since when there are no cells, nothing can be produced by them. Given these constraints, we use the following simple functional forms:

$$\text{Activator case:} \quad s(c) = k\frac{(h-1)c + hc_0}{2(h-1)c + c_0}, \qquad f(n) = \lambda c_0 \frac{n}{n_0}\left(\frac{n_0^2 + \alpha^2}{n^2 + \alpha^2}\right).$$

$$\text{Inhibitor case:} \quad s(c) = k\left(\frac{2c_m(h-\beta)c}{c_m^2 + c^2} + \beta\right), \quad f(n) = \frac{\lambda c_0}{n_0} n.$$

Here hk is the maximum value of $s(c)$, and α and c_m are positive constants, with $\beta = (c_m^2 - 2hc_0c_m + c_0^2)/(c_m - c_0)^2$.

The appropriate boundary conditions for the system (B.1) are $n = n_0$ and $c = c_0$ at the initial wound boundary. The solutions then have the form of waves of cells and chemical moving inwards to heal the wound. In one space dimension, corresponding to a linear slash wound, these wave forms are amenable to analysis as travelling waves, enabling bounds to be derived for the wave speed (Sherratt & Murray, 1991).

Acknowledgements

JAS was supported in part by a graduate studentship from the Science and Engineering Research Council of Great Britain, and in part by a Junior Research Fellowship at Merton College, Oxford. This work (JDM) was in part supported by grant DMS-900339 from the U.S. National Science Foundation. JAS would like to thank Dr Philip Maini and Robert Payne (Centre for Mathematical Biology, Oxford) for helpful discussions on the modelling aspects of this work.

This paper was read at the Sixth IMA Conference on the Mathematical Theory of the Dynamics of Biological Systems, held in Oxford, 1–3 July 1992.

References

Barrandon, Y., & Green, H. 1987 Cell migration is essential for sustained growth of keratinocyte colonies: The roles of transforming growth factor α and epidermal growth factor. *Cell* **50**, 1131–7.

Bershadsky, A., & Vasiliev, J. 1988 *Cytoskeleton.* New York: Plenum Press.

Buck, R. C. 1979 Cell migration in repair of mouse corneal epithelium. *Invest. Ophthalmol. Vis. Sci.* **18**, 767–84.

Chen, W. 1981 Mechanism of retraction of the trailing edge during fibroblast movement. *J. Cell Biol.* **90**, 187–200.

Clark, R. A. F. 1989 Wound repair. *Curr. Op. Cell Biol.* **1**, 1000–1008.

Coffey, R. J., Derynck, R., Wilcox, J. N., Bringman, T. S., Goustin, A. S., Moses, H. L., & Pittelkow, M. R. 1987 Production and auto-activation of transforming growth factor-α in human keratinocytes. *Nature* **328**, 817–20.

Crosson, C. E., Klyce, S. D., & Beuerman, R. W. 1986 Epithelial wound closure in the rabbit cornea. *Invest. Ophthalmol. Vis. Sci.* **27**, 464–73.

Danjo, S., Friend, J., & Throft, R. A. 1987 Conjunctival epithelium in healing of corneal epithelial wounds. *Invest. Ophthalmol. Vis. Sci.* **28**, 1445–9.

DiPasquale, A. 1975a Locomotory activity of epithelial cells in culture. *Exp. Cell Res.* **94**, 191–215.

DiPasquale, A. 1975b Locomotion of epithelial cells. Factors involved in extension of the leading edge. *Exp. Cell Res.* **95**, 425–39.

EISINGER, M., SADAN, S., SILVER, I. A., & FLICK, R. B. 1988 Growth regulation of skin cells by epidermal cell-derived factors: Implications for wound healing. *Proc. Natl. Acad. Sci. USA* **85**, 1937–41.

ELGJO, K., REICHELT, K. L., EDMINSON, P., & MOEN, E. 1986a Endogenous peptides in epidermal growth control. In: *Biological Regulation of Cell Proliferation* (R. Baserga, P. Foa, D. Metcalf, & E. E. Polli, eds.). New York: Raven Press, pp. 259–65.

ELGJO, K., REICHELT, K. L., HENNINGS, H., MICHAEL, D., & YUSPA, S. H. 1986b Purified epidermal pentapeptide inhibits proliferation and enhances terminal differentiation in cultured mouse epidermal cells. *J. Invest. Dermatol.* **87**, 555–8.

ELSON, E. L. 1988 Cellular mechanics as an indicator of cytoskeletal structure and function. *Ann. Rev. Biophys. Biophys. Chem.* **17**, 397–430.

FAULSTICH, E., TRISCHMANN, H., & MAYER, D. 1983 Preparation of trimethylrhodaminyl-phalloidin and uptake of the toxin into short-term cultured hepatocytes by endocytosis. *Exp. Cell Res.* **144**, 73–82.

FRANTZ, J. M., DUPUY, B. M., KAUFMAN, H. E., & BEUERMAN, R. W. 1989 The effect of collagen shields on epithelial wound healing in rabbits. *Am. J. Ophthalmol.* **108**, 524–8.

GABBIANI, G., CHAPPONIE, C., & HÜTTNER, I. 1989 Cytoplasmic filaments and gap junctions in epithelial cells and myofibroblasts during wound healing. *J. Cell Biol.* **76**, 561–8.

GERHART, J., & KELLER, R. 1986 Region-specific cell activities in amphibian gastrulation. *Ann. Rev. Cell Biol.* **2**, 201–29.

HALABAN, R., LANGDON, R., BIRCHALL, N., CUONO, C., BAIRD, A., SCOTT, G., MOELLMANN, G., & MCGUIRE, J. 1988 Basic fibroblast growth factor from human keratinocytes is a natural mitogen for melanocytes. *J. Cell Biol.* **107**, 1611–19.

HARRIS, A. K. 1982 Traction, and its relations to contraction in tissue cell locomotion. In: *Cell Behaviour* (R. Bellairs, A. Cirtus, & G. Dunn, eds.). Cambridge University Press, pp. 109–34.

HERGOTT, G. J., SANDIG, M., & KALNINS, V. I. 1989 Cytoskeletal organisation of migrating retinal pigment epithelial cells during wound healing in organ culture. *Cell Motil.* **13**, 83–93.

JANMEY, P. A., HVIDT, S., PEETERMANS, J., LAMB, J., FERRY, J. D., & STOGGEL, T. P. 1988 Viscoelasticity of F-actin and F-actin/gelsolin complexes. *Biochemistry* **27**, 8218–27.

KOLEGA, J. 1986 Effects of mechanical tension on protrusive activity and microfilament and intermediate filament organization in an epidermal epithelium moving in culture. *J. Cell Biol.* **102**, 1400–11.

KRAWCZYK, W. S. 1971 A pattern of epidermal cell migration during wound healing. *J. Cell Biol.* **49**, 247–63.

MADDEN, M. R., NOLAN, E., FINKELSTEIN, J. L., YURT, R. W., SMELAND, J., GOODWIN, C. W., HEFTON, J., & STAIANO-COICO, L. 1989 Comparison of an occlusive and a semi-occlusive dressing and the effect of the wound exudate upon keratinocyte proliferation. *J. Trauma* **29**, 924–31.

MARTIN, P., & LEWIS, J. 1991 The mechanics of embryonic skin wound healing—limb bud lesions in mouse and chick embryos. In: *Fetal Wound Healing: A Paradigm of Tissue Repair* (N. S. Adzick & M. T. Longaker, eds.). New York: Elsevier, pp. 265–79.

MARTIN, P., & LEWIS, J. 1992 Actin cables and epidermal movement in embryonic wound healing. *Nature*. In press.

MARTIN, P., HOPKINSON-WOOLLEY, J., & MCCLUSKEY, J. 1992 Growth factors and cutaneous wound repair. *Prog. Growth Factor Res.* In press.

MATTEY, D. L., & GARROD, D. R. 1984 Organization of extracellular matrix by chick embryonic corneal epithelial cells in culture and the role of fibronectin in adhesion. *J. Cell Sci.* **67**, 171–88.

MURRAY, J. D. 1989 *Mathematical Biology*. Berlin: Springer.

MURRAY, J. D., MAINI, P. K., & TRANQUILLO, R. T. 1988 Mechanochemical models for generating biological pattern and form in development. *Phys. Rep.* **171**, 59–84.

MURRAY, J. D., & OSTER, G. F. 1984 Generation of biological pattern and form. *IMA J. Math. Appl. Med. Biol.* **1**, 51–75.

OSTER, G. F. 1984 On the crawling of cells. *J. Embryol. Exp. Morphol.* **83** Suppl., 329–64.
OSTER, G. F., MURRAY, J. D., & HARRIS, A. K. 1983 Mechanical aspects of mesenchymal morphogenesis. *J. Embryol. Exp. Morphol.* **78**, 83–125.
OSTER, G. F., MURRAY, J. D., & ODELL, G. M. 1985 The formation of microvilli. In: *Molecular Determinants of Animal Form* (G. M. Edelman, ed.) New York: Alan R. Liss, pp. 365–84.
OSTER, G. F., & ODELL, G. M. 1984 Mechanics of cytogels. I: Oscillations in *Physarum. Cell Motil.* **4**, 469–503.
POLLARD, T. D. 1990 Actin. *Curr. Op. Cell Biol.* **2**, 33–40.
RADICE, G. 1980 The spreading of epithelial cells during wound closure in *Xenopus* larvae. *Dev. Biol.* **76**, 26–46.
SHAH, M., FOREMAN, D. M., & FERGUSON, M. W. J. 1992 Control of scarring in adult wounds by neutralising antibody to transforming growth factor β. *Lancet* **339**, 213–14.
SHERRATT, J. A. 1991 A perturbation problem arising from a mechanical model for epithelial morphogenesis. *IMA J. Appl. Math.* **47**, 147–62.
SHERRATT, J. A. 1992a Actin aggregation and embryonic epidermal wound healing. *J. Math. Biol.* In press.
SHERRATT, J. A. 1992b Cellular growth control and travelling waves of cancer. *SIAM J. Appl. Math.* In press.
SHERRATT, J. A., & LEWIS, J. 1992 Stress-induced alignment of actin filaments and the mechanics of cytogel. *Bull. Math. Biol.* In press.
SHERRATT, J. A., & MURRAY, J. D. 1990 Models of epidermal wound healing. *Proc. R. Soc. Lond.* B **241**, 29–36.
SHERRATT, J. A., & MURRAY, J. D. 1991 Mathematical analysis of a basic model for epidermal wound healing. *J. Math. Biol.* **29**, 389–404.
SHERRATT, J. A., & MURRAY, J. D. 1992a Epidermal wound healing: A theoretical approach. *Comm. Theor. Biol.* In press.
SHERRATT, J. A., MURRAY, J. D. 1992b Epidermal wound healing: The clinical implications of a simple mathematical model. *Cell Transplant.* In press.
SHERRATT, J. A., NOWAK, M. A. 1992 Oncogenes, anti-oncogenes and the immune response to cancer: A mathematical model. *Proc. R. Soc. Lond.* B **248**, 261–71.
STENN, K. S., & DEPALMA, L. 1988 Re-epithelialization. In: *The Molecular and Cellular Biology of Wound Repair* (R. A. F. Clark & P. M. Henson, eds.). New York: Plenum Press, pp. 321–35.
STOPAK, D., & HARRIS, A. K. 1982 Connective tissue morphogenesis by fibroblast traction. I: Tissue culture observations. *Dev. Biol.* **90**, 383–98.
TRINKAUS, J. P. 1984 *Cells into Organs. The Forces that Shape the Embryo.* Englewood Cliffs, NJ: Prentice-Hall.
VALBERG, P. A., & ALBERTINI, D. F. 1985 Cytoplasmic motions, rheology, and structure probed by a novel magnetic particle method. *J. Cell Biol.* **101**, 130–40.
VAUGHAN, R. B., & TRINKAUS, J. P. 1966 Movements of epithelial cell sheets *in vitro*. *J. Cell Sci.* **1**, 407–13.
WATT, F. M. 1988a Proliferation and terminal differentiation of human epidermal keratinocytes in culture. *Biochem. Soc. Trans.* **16**, 666–8.
WATT, F. M. 1988b The epidermal keratinocyte. *Bioessays* **8**, 163–7.
WECHEZAK, A. R., VIGGERS, R. F., & SAUVAGE, L. R. 1985 Fibronectin and F-actin redistribution in cultured endothelial cells exposed to shear stress. *Lab. Invest.* **53**, 639–47.
WECHEZAK, A. R., WIGHT, T. N., VIGGERS, R. F., & SAUVAGE, L. R. 1989 Endothelial adherence under shear stress is dependent upon microfilament reorganisation. *J. Cell Physiol.* **139**, 136–46.
WEINBERG, R. A. 1989 Growth factors and oncogenes. In: *Oncogenes and the Molecular Origins of Cancer* (R. A. Weinberg, ed.), Cold Spring Harbor, NY: Cold Spring Harbor Laboratory Press, pp. 45–66.
WHITBY, D. J., & FERGUSON, M. W. J. 1991 Immunohistochemical localisation of growth factors in fetal wound healing. *Dev. Biol.* **147**, 207–15.

WINSTANLEY, E. W. 1975 The epithelial reaction of the healing of excised cutaneous wounds in the dog. *J. Comp. Pathol.* **85**, 61–75.

WINTER, G. D. 1962 Formation of the scab and the rate of epithelialisation of superficial wounds in the skin of the young domestic pig. *Nature* **193**, 293–4.

WINTER, G. D. 1972 Epidermal regeneration studied in the domestic pig. In: *Epidermal Wound Healing* (H. I. Maibach & D. T. Rovee, eds.). Chicago: Year Book Medical Publishers, pp. 71–112.

WULF, E., DEBOBEN, A., BAUTZ, F. A., FAULSTICH, H., & WIELAND, T. 1979 Fluorescent phallotoxin, a tool for the visualization of cellular actin. *Proc. Natl. Acad. Sci. USA* **76**, 4498–4502.